Medical Engineering and Physics 124 (2024) 104097

Contents lists available at ScienceDirect

Medical Engineering and Physics

journal homepage: www.elsevier.com/locate/medengphy

Mechanical load applied by Intraosseous Transcutaneous Amputation Prosthesis (ITAP) during walking on level and sloped treadmill: A case study

K. Ahmed [a,b,*], M. Thornton [a,c], S.J.G. Taylor [a]

[a] Department of Orthopaedics and Musculoskeletal Science, Division of Surgery and Interventional Science, University College London, Brockley Hill, Stanmore, Middlesex, HA7 4LP, UK
[b] Center for Bionics and Pain Research, Mölndals Sjukhus, 431 30 Sweden
[c] Motor Learning Laboratory, Royal National Orthopaedic Hospital, Brockley Hill, Stanmore, Middlesex, HA7 4LP, UK

ARTICLE INFO

Keywords:
Amputation biomechanics
Bone-anchored prosthesis
Osseointegrated implant
Skeletally anchored amputation implant
Transfemoral kinetics
Intraosseous transcutaneous amputation prosthesis
Transfemoral bone anchor

ABSTRACT

This proof of concept study presents a method to collect and analyse kinetic data from one participant with a transfemoral amputation fitted with a percutaneous osseointegrated implant walking on a level and sloped treadmill. We describe the construction of and results from a bespoke wireless six axis load cell built into one participant's prosthetic assembly. The load cell does not clinically compromise the participant in any way and is an initial milestone in the development of a light-weight wireless load cell for use with percutaneous osseointegrated implants. In this case, it is the first time that kinetic data from a participant fitted with an Intraosseous Transcutaneous Amputation Prosthesis has been published. We propose that the data can be used to model the load transfer to the host bone, with several clinically significant applications. The raw dynamic data are made available and quasi-static load cases for each functional phase of gait are presented. Peak forces obtained in the medio-lateral (X), cranio-caudal (Y) and antero-posterior (Z) axes over level ground respectively were -243.8 N (0.24 BW), 1321.5 N (1.31 BW) and -421.8 N (0.42 BW); uphill were -141.0 N (0.14 BW), 1604.2 N (1.59 BW), -498.1 N (0.49 BW); downhill were -206.0 N (0.20 BW), 1103.9 N (1.09 BW), -547.2 N (0.54 BW). The kinetics broadly followed able bodied gait patterns with some gait strategies consistent in participants with other implant designs or prosthetic socket connections, for example offloading the artificial limb downhill.

1. Introduction

Spatiotemporal gait parameters in participants with unilateral transfemoral amputation (TFA) diverge from equivalent able bodied (AB) participants. For instance self selected walking speeds in TFA and AB populations range between 0.87 - 1.04 m s^{-1} and 1.36 - 1.45 m s^{-1} respectively and there is asymmetry in double stance time, step length and increased cost of gait energy [1,2]. The reasons for and degree of divergence is multifarious; research indicates that prosthetic components and alignment play a significant role [3]. We know less about how kinetic gait parameters differ between those with TFA and AB participants, part of the reason is a lack of data. Specialist environments or equipment such as gait labs or instrumented treadmills are necessary to collect kinetic data from untethered participants in six degrees of freedom (DOF). This presents a global challenge in relation to prosthetic services in low-resource settings [4]. A load cell close to the site of interest is another method to collect kinetic data, however with the exception of relatively expensive commercial devices such as those used by Frossard, Gow [5] and Niswander, Wang [6] these are often wired or may not record six DOF. A growing number [7] of individuals with TFA are being fitted with percutaneous osseointegrated implants (POI), as an alternative to prosthetic sockets [8], and it is important to understand the associated biomechanics. Reporting temporal gait parameters in POI for functional outcomes is valuable [9], and together with kinetic data is clinically significant in several ways:

Abbreviations: %GC, percentage of the gait cycle; BW, body weight; COM, centre of mass; ITAP, Intraosseous Transcutaneous Amputation Prosthesis; AB, able bodied; OPRA, Osseointegrated Prosthesis for the Rehabilitation of Amputees; POI, percutaneous osseointegrated implant; TFA, transfemoral amputation.

* Corresponding author at: Center for Bionics and Pain Research, Mölndals Sjukhus 431 30, Sweden.
E-mail address: kirstin@chalmers.se (K. Ahmed).

https://doi.org/10.1016/j.medengphy.2023.104097
Received 8 May 2023; Received in revised form 20 December 2023; Accepted 22 December 2023
Available online 5 January 2024

- Guiding prosthetic component choices to minimise wear and tear, mitigate for asymmetrical loading and possible component replacement.
- Development of control strategies for active artificial limbs using force thresholds as an input for control.
- Informing treatment and rehabilitation protocols to promote appositive bone remodelling and minimising endosteal resorption to optimise osseous interface stability [10–12] and mitigate for possible surgical revision.
- The design of POI (topology, material, and fixation choices) through targeted strain adaptive bone remodeling, i.e., to locally control apposition and resorption.

A POI connection between the residual femur and artificial limb transmits ground reaction force through the implant and femur directly. Factors that will affect load transfer through the implant/femur include anthropomorphic features, residual limb length [13], those which influence ambulatory technique [14] such as prosthetic components or pain, and POI design [15]. Some gait kinetic reference values for TFA participants with prosthetic sockets is available [2] and there is some POI kinetic literature, mainly for the Osseointegrated Prosthesis for the Rehabilitation of Amputees (OPRA) system, [16–19]. The OPRA is a threaded, hollow, intramedullary fixture made of a Titanium alloy (TiAl6V4) with a percutaneous abutment that connects to an artificial leg. In OPRA studies, authors used a commercially available wireless six axis load cell (iPecs Lab system, RTC electronics, United States) interposed between the residual limb and artificial leg of 12 participants to record data. The data set has been used in several publications employing the Finite Element (FE) method [20,21], multi body simulations, development of prosthetic components [22], and the analysis of POI materials [23,24]. Moreover, the data was recollected from OPRA participants ten years later, in 2017 [25] with the same load cell from five participants (some of whom may have been part of the original 12). It is apparent that this data set holds value to the research field, yet there are very few similar data sets or data acquisition methods available with other POI designs in participants with TFA. It is important to add to this data set and in preliminary steps towards this goal, this study collects level and sloped treadmill gait kinetic data in a participant with a TFA using the Intraosseous Transcutaneous Amputation Prosthesis (ITAP) system. The ITAP is a press fit solid stemmed intramedullary POI, sometimes cemented, with a radial ''collar'' on which the osteotomy interfaces with. It is made of TiAl6V4 and has a percutaneous spigot that connects to an artificial leg.

Currently, POI are sized on an individual basis from a core proprietary design specific to each manufacturer or research group. We propose that an open source database of design linked POI kinetic profiles collated under consistent testing standards will inform future POI design and ensure meritorious bone remodeling [17]. Our objectives were to develop an affordable, lightweight, wireless, and easy to fit device to measure directly the mechanical constraints applied by the ITAP onto the host bone. We built the load cell into the participant's prosthetic assembly and report the construction and results. Raw dynamic data are available from DOI:10.17632/sks3d6sd6f.1 and quasi-static load cases for each functional phase of gait are presented.

2. Materials and methods

2.1. Participant information

The participant was a 50 year old male with a left transfemoral amputation (residuum = 181 mm measured from greater trochanter proximal ridge) as a result of a trauma incurred aged 18, he provided full informed consent for this study. He had used a prosthetic socket until he received an ITAP in 2012 as part of a clinical trial (Identifier = NCT02491424). The ITAP spigot connected to a failsafe release device which protects the bone from overload (MKII, Stanmore Implants Worldwide, UK). The failsafe connected to a microprocessor controlled Genium knee, which in turn was attached to a mechanical carbon fibre Taleo foot (both Ottobock, Duderstadt, Germany) using standard prosthetic fittings. He was 1.89 m tall and weighed 102.8 kg (including the 3.3 kg artificial leg and all prosthetic components) with a K3 prosthetic activity level.

2.2. Load cell construction

A prosthetic tube connecting the artificial knee and failsafe device was replaced with an instrumented titanium tube (forming the load cell). Thin film strain gauges located on each of four sides (20 kOhms) were fabricated on each of four orthogonal flat sides milled into the outer surface. Gauges were wire bonded to a flexible printed circuit which interconnected the four quadrants. Electrically, these formed four half bridges of gauges wired for primary sensitivity to axial compression, AP bending and ML bending. Four gauges at 45 ° to the long axis were wired into four channels of quarter bridge action only, for primary sensitivity to AP and ML shear forces and torque. It was accepted that there would be crosstalk between channels wired primarily for one DOF, as is usually the case where gauges are shared between DOF's, and the matrix method of calibration was therefore used to identify and appropriately combine channels sensitive to more than one applied load type. Each channel was wired to a printed circuit for amplification, A-D conversion, serial data streaming and radio transmission and the instrumentation was powered by a LiPo battery. Each strain gauge half bridge was wired to one channel of a 24 bit analog input microcontroller/A-D converter, and these combined to produce a serial data stream of numbers proportional to strain (strain counts), sampling each strain channel at 50 samples/*sec*; this was fed to a UHF sub-GHz radio transmitter for reception by a LabView program on the host computer in real time. A thin plastic collar provided protection for the gauges without adding to the stiffness. See Fig. 1.

2.3. Fitting and alignment

The distal and proximal faces of the failsafe and artificial knee respectively incorporated male pyramid plates. We attached the load cell between these plates with female pyramid fittings and tightened with grub screws to 15 Nm. The load cell was designed to exactly replicate the dimensions of the prosthetic tube it replaced being 74 mm itself plus fittings to occupy the 110 mm vertical height space. There was negligible weight/inertial change, and it was fitted by an experienced ITAP prosthetist to ensure there was no deviation from the participant's previous alignment. Axes were medio-lateral (X), cranio-caudal (Y) and antero-posterior (Z), see Fig. 2.

2.4. Load cell calibration and load vector output

The load cell was calibrated directly after the clinical session, taking account of adjustments made just prior to the data collection such as the interlock of the prosthetic fittings. During calibration, loads were applied to the construct as follows: Axial force was applied using a Hounsfield uniaxial compression rig with balls between load centres and the pyramid fittings; loads were applied to 1.25 kN in 100 N steps. Bending and shear were applied using cantilever loading, bending and shear contributions of strain being separated by loading at two lever arms. Torque was applied using a torque rig comprising a bending bar with pulleys, cord, and deadweight for pure torque application. Sensitivities of each strain channel to each applied load were found (8 × 6). Channels were then combined according to their primary contribution to each applied load, and these resulting six combined channels vs. the six DOF formed the six-by-six calibration matrix, representing the sensitivities and cross-sensitivities of each combination of strain channels to each pure load type, in counts/N and counts/Nm. Inverting the calibration matrix produced the measurement matrix having units of N/

Fig. 1. (a): Prosthetic tubing before load cell replacement. (b) Load cell with one flat and gold wires on a flexible circuit pad before and then after fitting the protective plastic collar and wired to electronics. (c) Final assembly with load cell replacing prosthetic tubing.

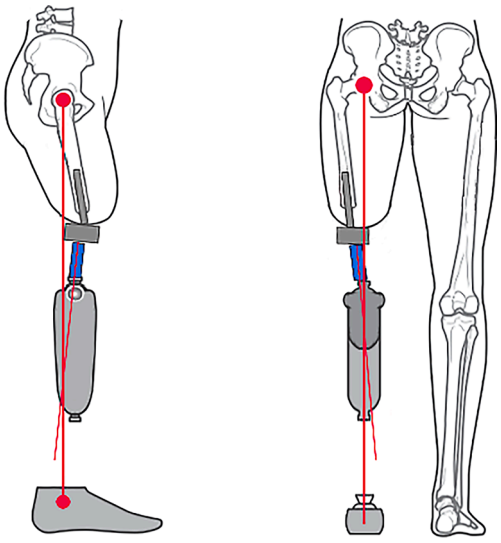

Fig. 2. Illustration of medial view of left leg and posterior view of subject showing the POI, failsafe, loadcell (blue), prosthetic knee and foot.

count and Nm/count. Upon multiplying this measurement matrix by each measured strain count vector, and eliminating the strain count offsets, corresponding to zero applied load, produced the 6 DOF load vector. The calibration matrix calculations were carried out in Excel, and the measurement matrix stored in a LabView GUI. As a check, the measurement matrix was applied to the original raw data used in the static calibration. Channel combination and RMSE is provided in Tables 3 and 4 of the supplemental material.

2.5. Kinetic data collection

Uphill, level, and downhill gait data was collected on a treadmill (GRAIL Motek, Amsterdam, The Netherlands). After fitting the load cell, the participant acclimatised to the treadmill conditions for 20 min during which time he self-selected comfortable walking speeds and gradients. The uphill and downhill gradients were selected at 8.5 ° and 7.0 ° respectively. Level and downhill walking was comfortable at 1.0 m/s; uphill walking was selected at 0.8 m/s. The load cell strain counts were measured under 'no load' conditions with the device fitted in situ, and these were used to provide a known zero load for the calibration. The participant walked untethered and without the use of handrails, the entire session was approximately 45 min with several breaks.

2.6. Walking cycle data separation and processing

Two minutes of data were collected during each walking trial (6000 data samples) and a standard method of processing was used. There were 87, 71, and 78 gait cycles in level, uphill and downhill walks respectively after removing traces resulting from errors in transmission (very obvious large spikes in F_y traces). Gait cycles representing an atypical gait ($>$ 1.5 SD from the mean), were also removed leaving 46, 49, and 14 level, uphill and downhill gait cycles respectively. The raw strain counts were first filtered by a biorthogonal wavelet filter which reduced the effective sampling frequency to 20 Hz; this preserved the essential frequency content of each sample. After conversion of the raw counts to forces and moments each gait cycle was defined between ipsilateral heel strikes identified by the axial force component (F_y in the cranio-caudal axis). Toe off in terminal stance was identified when the ipsilateral foot left the ground in advance of the initial swing phase $F_y \leq 0$ and remade contact in advance of the initial contact phase at $F_y \geq 0$. The cyclic data signals were time normalised using an algorithm developed in Excel which either compressed or expanded each gait cycle so that 0 and 100 % of every trace were colinear with a representative gait cycle (identified visually using the literature [2]). The mean and standard deviation (SD) of the time-normalised gait cycles were calculated. This method is consistent with those in the literature [26]. Resultant gait cycles were then used to calculate the new mean. Note that force and moments are reported with respect to the participant's leg.

2.7. Functional phases of gait

The data points for the functional phases of gait were identified using the literature [27,28]:

1. Initial contact (heel strike) described as the moment the foot just touches the floor and the immediate reaction to the onset of body weight transfer.
2. Loading response (foot flat) where body weight is transferred to the leading limb until the contralateral limb is lifted.
3. Mid-stance is the first part of single leg stance where the trailing leg (contralateral limb) is lifted and advances over stationary foot until body weight is aligned over the forefoot.
4. Terminal stance (heel off) is the second part of single leg stance beginning with heel rise.
5. Initial swing (toe off) also called pre swing starts with initial contact of the contralateral limb and ends with ipsilateral toe off.

3. Results

3.1. Individual data charts

We plotted 46, 49, and 14 level, uphill and downhill respectively sloped walks. Load cell forces and moments for level treadmill walking at 1.0 m/s are plotted across one gait cycle in Figs. 3a and b. All raw data, after calibration and load vector output, is available at DOI:10.17632/sks3d6sd6f.1

3.2. Averaged data charts

The mean trace for each DOF in level and sloped treadmill walking is presented with vertical axes normalised with body mass (including prosthesis) in Figs. 4a – c and Table 1.

3.3. Forces representative of the functional phases of gait

Using mean trace data, a set of forces and moments representing the stance phases of the gait cycle at the load cell were produced over level and sloped treadmill walking and are presented in Table 2. The average mid stance onset was ~40% GC and terminal stance was ~50%. Peak forces obtained in X, Y and Z axes over level ground respectively were −243.8 N (0.24 BW), 1321.5 N (1.31 BW) and −421.8 N (0.42 BW); uphill were −141.0 N (0.14 BW), 1604.2 N (1.59 BW), −498.1 N (0.49 BW); downhill were −206.0 N (0.20 BW), 1103.9 N (1.09 BW), −547.2 N (0.54 BW).

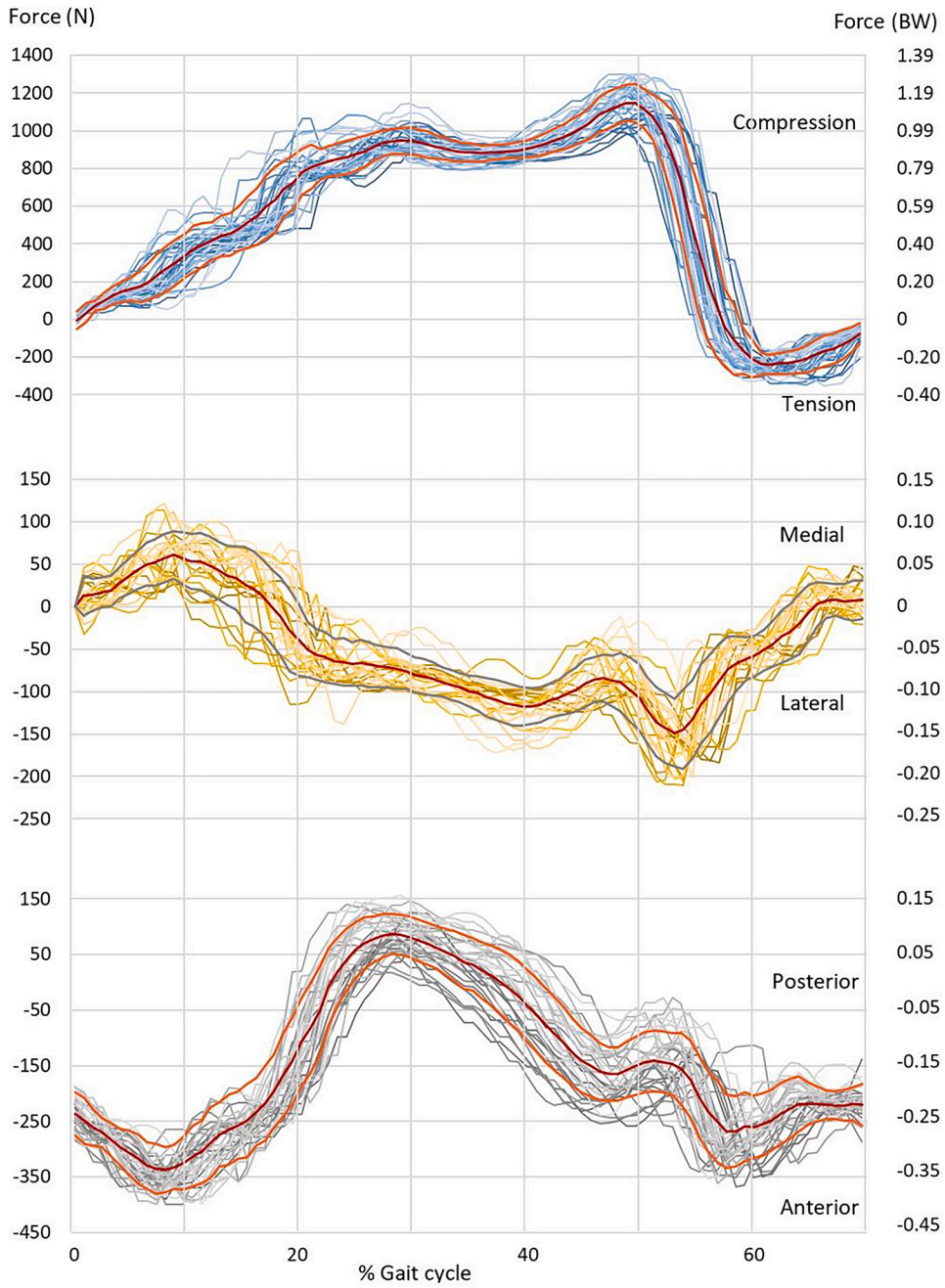

Fig. 3a. (a): Processed Forces (N) in 87 gait cycles. Level treadmill walking at 1.0 m/s. Mean (red) +/- 1 SD (orange/grey). Top: Axial (F_y), Middle: ML shear (F_x), Bottom: AP shear (F_z).

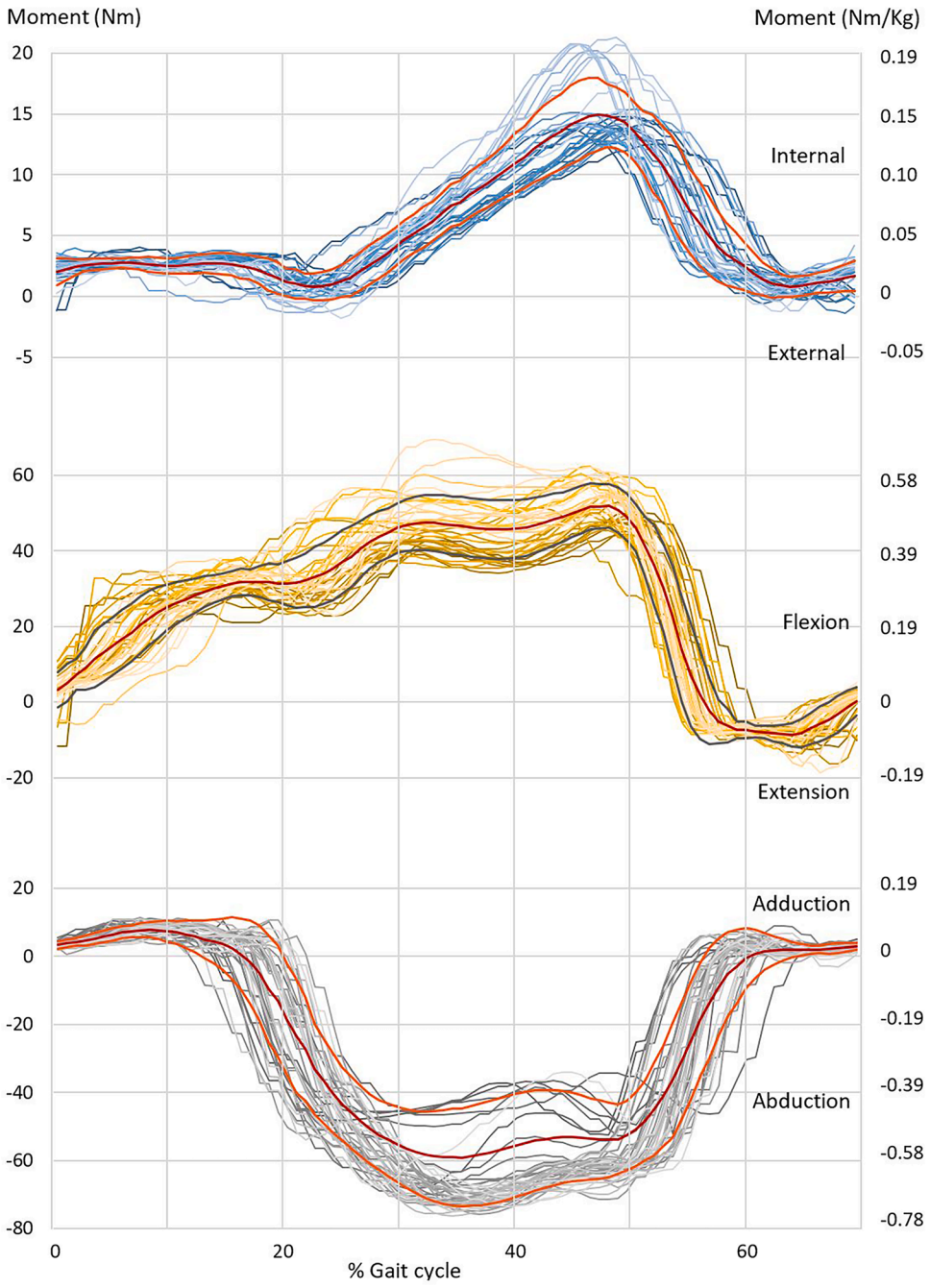

Fig. 3b. (b): Processed Moments (Nm) in 87 gait cycles. Level treadmill walking at 1.0 m/s. Mean (red) +/- 1 SD (orange/grey). Top: Axial torque (M_y), Middle: bending around ML axis (M_x), Bottom: bending around AP axis (M_z).

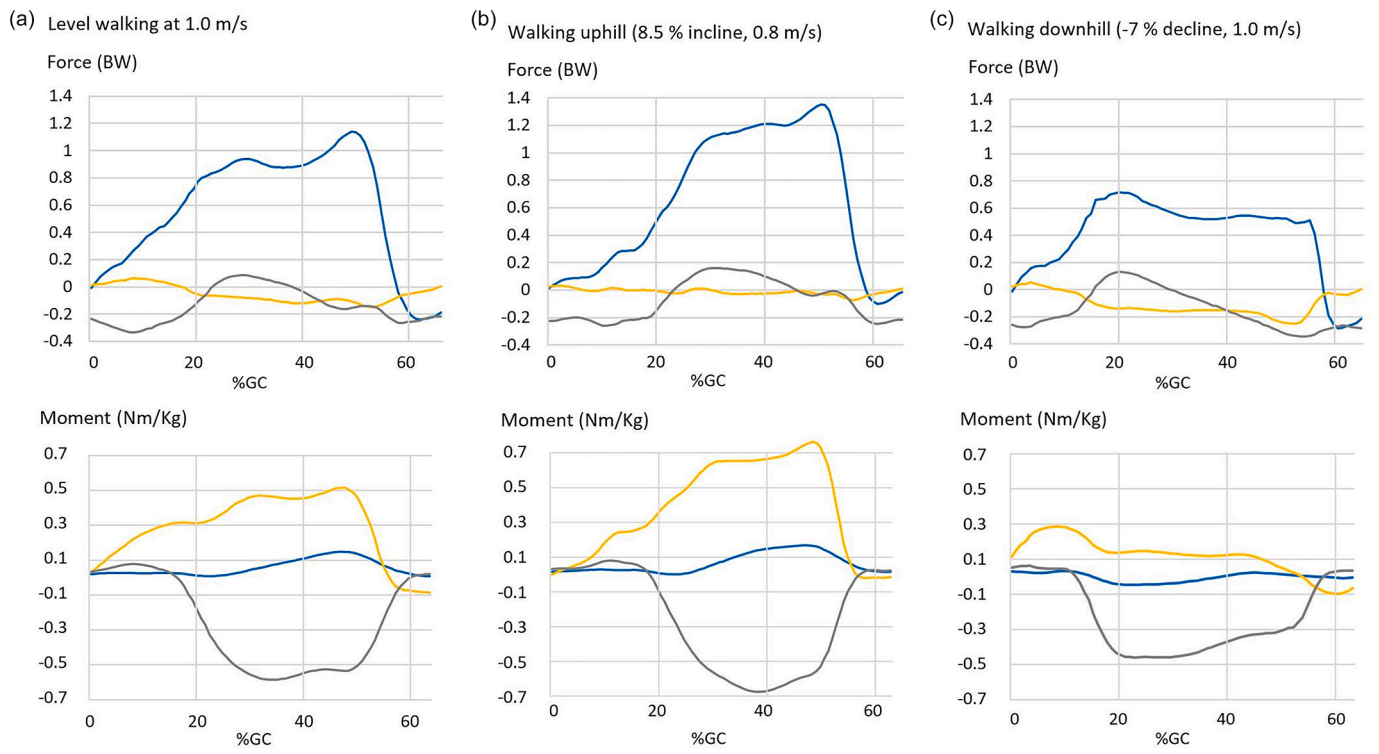

Fig. 4. (a): Mean level walking at 1.0 m/s from 46 gait cycles. Initial contact (heel strike) = ~30% GC, Initial swing (toe off) = ~50% GC. (b): Mean walking uphill (8.5% incline, 0.8 m/s) from 49 gait cycles. Initial contact (heel strike) = ~30% GC, Initial swing (toe off) = ~50% GC. (c): Mean walking downhill (−7% decline, 1.0 m/s) from 14 gait cycles. Initial contact (heel strike) = ~20% GC, Initial swing (toe off) = ~50% GC
Key: Positive forces = Compression (F_y), Medial (F_x), Posterior (F_z). Positive moments = Internal torque (M_y), Flexion (M_x), Abduction (M_z). Blue = F_y, M_y. Yellow = F_x, M_x. Grey = F_z, M_z.

Table 1
Standard deviation (SD) and Coefficient of Variance (COV) of the mean for all forces and moments in level and sloped treadmill walking.

Slope		F_x	F_y	F_z	M_x	M_y	M_z
Level	SD	53.4 (0.05)	440.3 (0.44)	−110.5 (0.11)	−19.3 (−0.19)	5.40 (0.05)	25.5 (0.25)
	COV	−1.72	1.03	0.71	0.80	0.95	−1.50
Uphill	SD	20.4 (0.02)	520.3 (0.52)	160.0 (0.16)	29.8 (0.29)	6.1 (0.06)	32.7 (0.32)
	COV	−1.90	0.79	1.97	0.81	0.98	−1.03
Downhill	SD	84.6 (0.08)	307.1 (0.30)	126.6 (0.13)	10.4 (0.10)	2.21 (0.02)	20.5 (0.20)
	COV	−1.02	0.79	−39.66	0.92	5.61	−0.85

Axes are Medio-lateral (X), Cranio-caudal (Y), Antero-posterior (Z).
Standard deviations are presented as absolute forces (N) or moments (Nm) with BW or Nm/Kg respectively, in brackets.

Table 2
Forces and moments in stance and initial swing in level and slope walking.

Slope	Functional phase of gait	F_x		F_y		F_z		M_x		M_y		M_z	
Level	Initial contact	18.2	(0.02)	34.3	(0.03)	−249.2	(−0.25)	5.1	(0.05)	2.2	(0.02)	3.8	(0.04)
	Loading response [1]	−80.1	(−0.08)	946.8	(0.94)	85.1	(0.08)	44.7	(0.44)	3.5	(0.03)	−53.9	(−0.52)
	Mid stance	−118.7	(−0.12)	887.0	(0.88)	0.0	(0)	45.7	(0.44)	9.3	(0.09)	−57.6	(−0.56)
	Terminal stance [2]	−108.3	(−0.11)	1147.0	(1.14)	−156.9	(−0.16)	50.8	(0.49)	14.7	(0.14)	−53.7	(−0.52)
	Initial swing	−24.2	(−0.02)	−231.3	(−0.23)	−227.8	(−0.23)	−8.5	(−0.08)	0.9	(0.01)	1.9	(0.02)
Uphill	Initial contact	26.0	(0.03)	16.8	(0.02)	−228.0	(−0.23)	−0.1	(0)	1.6	(0.02)	3.2	(0.03)
	Loading response	−16.5	(−0.02)	1143.9	(1.13)	161.2	(0.16)	65.3	(0.64)	6.2	(0.06)	−57.6	(−0.56)
	Mid stance	−26.3	(−0.03)	1208.4	(1.2)	124.2	(0.12)	66.1	(0.64)	13.0	(0.13)	−67.6	(−0.66)
	Terminal stance	−29.7	(−0.03)	1361.8	(1.35)	−30.2	(−0.03)	77.0	(0.75)	16.7	(0.16)	−57.7	(−0.56)
	Initial swing	−24.2	(−0.02)	−101.8	(−0.1)	−249.4	(−0.25)	−2.0	(−0.02)	2.5	(0.02)	2.3	(0.02)
Downhill	Initial contact	21.0	(0.02)	−11.9	(−0.01)	−259.8	(−0.26)	11.5	(0.11)	2.9	(0.03)	5.3	(0.05)
	Loading response	−140.9	(−0.14)	723.9	(0.72)	135.6	(0.13)	13.7	(0.13)	−4.1	(−0.04)	−43.8	(−0.43)
	Mid stance	−150.6	(−0.15)	526.4	(0.52)	−137.8	(−0.14)	12.0	(0.12)	−0.4	(0)	−39.5	(−0.38)
	Terminal stance	−253.8	(−0.25)	509.3	(0.51)	−339.9	(−0.34)	4.5	(0.04)	1.4	(0.01)	−30.5	(−0.3)
	Initial swing	−33.3	(−0.03)	−287.3	(−0.28)	−274.3	(−0.27)	−9.3	(−0.09)	−0.2	(0)	2.3	(0.02)

Axes are Medio-lateral (X), Cranio-caudal (Y), Antero-posterior (Z).
Kinetic data are presented as absolute forces (N) or moments (Nm) with BW or Nm/Kg respectively, in brackets.
[1] Load is recorded at the end of this phase (~ first axial force peak).
[2] Load is recorded at the end of this phase (~ second axial force peak).

4. Discussion

To be fitted with a POI, several inclusion criteria must be met and the vast majority of TFAs are not suitable [29]. The methods used in this study were different from those used in the OPRA data collection; we considered that the load cell did not influence the weight/inertial properties of the participants prosthetic assembly nor physically obstruct motion during gait and ensured the failsafe remained in situ. Although retaining the failsafe meant that the load cell was slightly more distal compared to replacing the failsafe this did not influence data validity whilst simultaneously mitigating a significant clinical risk. In the methods proposed, only one ITAP participant had enough vertical space (110 mm) to accommodate the necessary components, possibly because of his height (1.89 m), and this is a recognised drawback of our method. To address this, we propose to develop a lower profile load cell in future work rather than replacing the failsafe with a load cell as has been done with OPRA data collection [18,25].

There was a sizable difference between the anterior (braking) and posterior (propulsive) impulses when the area under the force-time curves were visually compared. This observation would have been compensated for by adjustments to stride length and stance time, since data was collected at a constant treadmill speed and may be due to the treadmill belt carrying the driving limb backwards in toe off. Mediolaterally, the ITAP participant experienced a lateral force in stance, also observed in AB gait and due to shifting the centre of mass (COM) over the supporting limb in double stance. This shift requires the remaining abductors to support the body weight (BW) [30], which in turn exerts a lateral force on the limb. Similarly, amongst prosthetic socket users, an increase in the applied lateral force in *both* limbs has been observed [31].

In the absence of hamstring and quadriceps muscular control, it is not possible for participants with TFA to prevent knee bucking in midstance (full weight bearing) [32]. A strategy to allow the movement of the COM without collapse is usually achieved with an artificial limb *stance yielding function* which is a type of midstance lock out. This mechanism is employed by the Genium knee that the ITAP patient used and may explain the very definite knee flexion moment throughout the entire stance phase (including initial loading). Downhill walking in AB increases limb loading [33] and requires controlled lowering of the COM, however an artificial limb may not be able to perform this. TFA participants with prosthetic sockets typically resolve this by relying more on the intact limb [34,35] thereby offloading the artificial limb as was observed in this study and in the OPRA data. The ITAP data results in similarities with AB gait patterns and phasing, although the first vertical force peak was < 1 BW and the midstance magnitude was $\sim$ 0.88 BW indicating a less dynamic gait than AB participants [36] (a dynamic gait has a greater excursion of the COM). This observation has also been noted in participants with TFA using prosthetic sockets [37], moreover, diminished data peaks compared to overground walking may be the effect of the treadmill [38], both observations require further work with matched controls to clarify the biomechanical picture.

4.1. Limitations and future work

The main limitation of this study was that data from only one participant, who was tall and not representative of a normal TFA population, a lower profile load cell (reduced vertical height) to collect data from more ITAP participants with different prosthetic components would enable a broader picture. In future work data should be collected both overground and, on a treadmill, using matched controls to observe the effects, if any, on the kinetic data. A valuable extension of this study would be to increase the SD in the filtering of the raw kinetic data to achieve a stronger assessment of variability (e.g., inter-step variability). Further future work might cross validate synchronised kinetic data sets collected using this load cell and embedded force plates in the laboratory and state-of-the-art portable kinetic systems outside the laboratory. Thereafter, we will move towards prospective clinical studies with aims to better understand implant stability criteria considering integration at the implant/bone interface, and POI designs. We anticipate the kinetic database will highlight the relationship between host bone strains and prosthetic component combinations and offer scalable force threshold control recommendations for active artificial limbs. Finally, a complete biomechanical picture with the addition of temporal and kinematic information will be useful in the refinement of clinical or rehabilitation protocols. It is hoped that results from these studies will help identify adverse events leading to aseptic or septic loosening which may ultimately relieve health care provision [39].

5. Conclusion

We have demonstrated the construction and collection of kinetic data in one participant fitted with an ITAP at the transfemoral level for the first time. The kinetics broadly followed AB gait patterns with some gait strategies consistent in participants with other implant designs or prosthetic socket connections, for example offloading the artificial limb downhill. This is an initial milestone in the development of future affordable light-weight wireless load cells. We have shown that without compromising safety nor altering gait, that it is possible to collect and extract kinetic data using a custom-made load cell compatible with prosthetic components. In order to produce a clinically meaningful kinetic database we must develop a lower profile load cell to fit a broader POI population and ensure the cross-validation of loading measurements. We encourage other researchers to replicate this study to build on the data repository.

Funding

None

Ethical approval

HRA ethical approval was obtained for this study (IRAS project ID = 226799, REC reference = 17/LO/1508)

CRediT authorship contribution statement

K. Ahmed: Conceptualization, Methodology, Formal analysis, Data curation, Writing – original draft. **M. Thornton:** Methodology, Formal analysis, Data curation, Writing – review & editing. **S.J.G. Taylor:** Conceptualization, Methodology, Writing – review & editing, Supervision.

Declaration of competing interest

None.

Acknowledgments

Authors would like to acknowledge the academic support of Professor Gordon Blunn (Portsmouth University, UK) and Professor Max Ortiz (Bionics Institute, Australia).

Supplementary materials

Supplementary material associated with this article can be found, in the online version, at doi:10.1016/j.medengphy.2023.104097.

References

[1] Mengelkoch LJ, Kahle JT, Highsmith MJ. Energy costs and performance of transfemoral amputees and non-amputees during walking and running: a pilot study. Prosthet Orthot Int 2017;41:484–91.

[2] Schmid-Zalaudek K, Fischer T, Szava Z, Lackner HK, Kropiunig U, Bittner C, et al. Kinetic gait parameters in unilateral lower limb amputations and normal gait in able-bodied: reference values for clinical application. J Clin Med 2022:11.
[3] Varrecchia T, Serrao M, Rinaldi M, Ranavolo A, Conforto S, De Marchis C, et al. Common and specific gait patterns in people with varying anatomical levels of lower limb amputation and different prosthetic components. Hum Mov Sci 2019; 66:9–21.
[4] Chadwell A, Diment L, Micó-Amigo M, Morgado Ramírez DZ, Dickinson A, Granat M, et al. Technology for monitoring everyday prosthesis use: a systematic review. J Neuroeng Rehabil 2020;17:93.
[5] Frossard L, Gow DL, Hagberg K, Cairns N, Contoyannis B, Gray S, et al. Apparatus for monitoring load bearing rehabilitation exercises of a transfemoral amputee fitted with an osseointegrated fixation: a proof-of-concept study. Gait Posture 2010;31:223–8.
[6] Niswander W, Wang W, Baumann AP. Characterizing loads at transfemoral osseointegrated implants. Med Eng Phys 2020;84:103–14.
[7] Tropf JG, Potter BK. Osseointegration for Amputees: current State of Direct Skeletal Attachment of Prostheses. Orthoplastic Surgery 2023.
[8] Handford C, McMenemy L, Kendrew J, Mistlin A, Akhtar MA, Parry M, et al. Improving outcomes for amputees: the health-related quality of life and cost utility analysis of osseointegration prosthetics in transfemoral amputees. Injury 2022;53: 4114–22.
[9] Frossard L, Hagberg K, Häggström E, Gow DL, Brånemark R, Pearcy M. Functional outcome of transfemoral amputees fitted with an osseointegrated fixation: temporal gait characteristics. JPO: J Prosthetics Orthotics 2010;22:11–20.
[10] Huiskes R, Weinans H, Grootenboer HJ, Dalstra M, Fudala B, Slooff TJ. Adaptive bone-remodeling theory applied to prosthetic-design analysis. J Biomech 1987;20: 1135–50.
[11] Mellal A, Wiskott HW, Botsis J, Scherrer SS, Belser UC. Stimulating effect of implant loading on surrounding bone. Comparison of three numerical models and validation by in vivo data. Clin Oral Implants Res 2004;15:239–48.
[12] Berg D, Frossard L. Health service delivery and economic evaluation of limb lower bone-anchored prostheses: a summary of the queensland artificial limb service's experience. Can Prosthet Orthot J 2021;4:36210.
[13] Bell JC, Wolf EJ, Schnall BL, Tis JE, Tis LL, Potter BK. Transfemoral amputations: the effect of residual limb length and orientation on gait analysis outcome measures. J Bone Joint Surg Am 2013;95:408–14.
[14] Adamczyk PG, Kuo AD. Mechanisms of gait asymmetry due to push-off deficiency in unilateral amputees. IEEE Trans Neural Syst Rehab Eng 2014;23(5):776–85.
[15] Ahmed K. ITAP: clinical outcomes and implant design optimisation using numerical modelling: UCL (Doctoral thesis); 2021 https://discovery.ucl.ac.uk/id/eprint/10137265/.
[16] Lee WC, Frossard LA, Hagberg K, Haggstrom E, Gow DL, Gray S, et al. Magnitude and variability of loading on the osseointegrated implant of transfemoral amputees during walking. Med Eng Phys 2008;30:825–33.
[17] Frossard L. Loading characteristics data applied on osseointegrated implant by transfemoral bone-anchored prostheses fitted with basic components during daily activities. Data Brief 2019;26:104492.
[18] Lee WC, Frossard LA, Hagberg K, Haggstrom E, Branemark R, Evans JH, et al. Kinetics of transfemoral amputees with osseointegrated fixation performing common activities of daily living. Clin Biomech (Bristol, Avon) 2007;22:665–73.
[19] Thesleff A, Häggström E, Tranberg R, Zügner R, Palmquist A, Ortiz-Catalan M. Loads at the implant-prosthesis interface during free and aided ambulation in osseointegrated transfemoral prostheses. IEEE Trans Med Robot Bionics 2020;2: 497–505.
[20] Tomaszewski PK, Verdonschot N, Bulstra SK, Verkerke GJ. A comparative finite-element analysis of bone failure and load transfer of osseointegrated prostheses fixations. Ann Biomed Eng 2010;38:2418–27.
[21] Prochor P, Frossard L, Sajewicz E. Effect of the material's stiffness on stress-shielding in osseointegrated implants for bone-anchored prostheses: a numerical analysis and initial benchmark data. Acta Bioeng Biomech 2020;22:69–81.
[22] Pather S. Design of a safety device to address the loading concerns of bone-anchored prostheses (Doctoral dissertation. Queensland University of Technology). Queensland University of Technology; 2019.
[23] Pitkin M, Pilling J, Raykhtsaum G. Mechanical properties of totally permeable titanium composite pylon for direct skeletal attachment. J Biomed Mater Res B Appl Biomater 2012;100:993–9.
[24] Thesleff A, Ortiz-Catalan M, Branemark R. Low plasticity burnishing improves fretting fatigue resistance in bone-anchored implants for amputation prostheses. Med Eng Phys 2022;100:103755.
[25] Stenlund P, Trobos M, Lausmaa J, Branemark R, Thomsen P, Palmquist A. Effect of load on the bone around bone-anchored amputation prostheses. J Orthop Res 2017;35:1113–22.
[26] Frossard L, Haggstrom E, Hagberg K, Branemark R. Load applied on bone-anchored transfemoral prosthesis: characterization of a prosthesis-a pilot study. J Rehabil Res Dev 2013;50:619–34.
[27] Jacquelin Perry M. Gait analysis: normal and pathological function. New Jersey: SLACK; 2010.
[28] Schmid-Zalaudek K, Fischer T, Száva Z, Lackner HK, Kropiunig U, Bittner C, et al. Kinetic gait parameters in unilateral lower limb amputations and normal gait in able-bodied: reference values for clinical application. J Clin Med 2022;11:2683.
[29] Smith D-F, Scott H, Hebenton J. The Scottish physiotherapy amputee research group annual report (2015). Physiotherapy 2019;105:e127–e8.
[30] Liu MQ, Anderson FC, Schwartz MH, Delp SL. Muscle contributions to support and progression over a range of walking speeds. J Biomech 2008;41:3243–52.
[31] Carse B, Scott H, Brady L, Colvin J. A characterisation of established unilateral transfemoral amputee gait using 3D kinematics, kinetics and oxygen consumption measures. Gait Posture 2020;75:98–104.
[32] Schmitz RJ, Harrison D, Wang H-M, Shultz SJ. Sagittal-plane knee moment during gait and knee cartilage thickness. J Athl Train 2017;52:560–6.
[33] Taylor SJG, Walker PS. Forces and moments telemetered from two distal femoral replacements during various activities. J Biomech 2001;34:839–48.
[34] Morgenroth DC, Roland M, Pruziner AL, Czerniecki JM. Transfemoral amputee intact limb loading and compensatory gait mechanics during down slope ambulation and the effect of prosthetic knee mechanisms. Clinical Biomechanics 2018;55:65–72.
[35] Debbi EM, Bernfeld B, Herman A, Laufer Y, Greental A, Sigal A, et al. Frontal plane biomechanics of the operated and non-operated knees before and after unilateral total knee arthroplasty. Clinical Biomechanics 2015;30:889–94.
[36] Soutas-Little RW. Motion Analysis and Biomechanics. J Rehabil Res Dev 1998: 49–68.
[37] Grimmer M, Seyfarth A. Mimicking human-like leg function in prosthetic limbs. Neuro-Robotics: Springer; 2014. p. 105–55.
[38] Riley PO, Paolini G, Della Croce U, Paylo KW, Kerrigan DC. A kinematic and kinetic comparison of overground and treadmill walking in healthy subjects. Gait Posture 2007;26:17–24.
[39] Soares Dos Santos MP, Bernardo RMC. Bioelectronic multifunctional bone implants: recent trends. Bioelectron Med 2022;8:15.